Selective EGF-Receptor deletion in myeloid cells limits atherosclerosis

Condensed title: Myeloid EGF-R deletion reduces atherosclerosis

Lynda Zeboudj[1], Andréas Giraud[1], Lea Guyonnet[1], Yujiao Zhang[1], Ludivine Laurans[1], Bruno Esposito[1], Jose Vilar[1], Anna Chipont[1], Nikolina Papac-Milicevic[2], Christoph J. Binder[2], Alain Tedgui[1], Ziad Mallat[1,3], Pierre-Louis Tharaux[1] & Hafid Ait-Oufella[1,4]

[1]Inserm U970, Paris Cardiovascular Research Center, Paris, France, Université René Descartes Paris 5

[2]Center for Molecular Medicine (CeMM) of the Austrian Academy of Sciences and Department of Laboratory Medicine, Medical University of Vienna, 1090 Vienna, Austria

[3]Department of Medicine, Division of Cardiovascular Medicine, University of Cambridge, Cambridge, UK.

[4]Service de Réanimation Médicale, Hôpital Saint-Antoine, AP-HP, Université Pierre-et-Marie Curie, Paris 6.

Conflict of interest: none

*Correspondence to Hafid Ait-Oufella, Inserm U970, Paris Cardiovascular Research Center, 56, rue Leblanc Paris, France, Université René Descartes Paris 5,

e mail: hafid.aitoufella@inserm.fr

Abstract

Objectives. To determine the consequences of specific inhibition of Epidermal Growth Factor Receptor (EGFR) in myeloid cells in atherosclerosis development.

Approach and Results. Atherosclerotic lesion size was significantly reduced in irradiated *Ldlr*$^{-/-}$ mice reconstituted with *LysM*$^{Cre+}$*Egfr*$^{lox/lox}$ bone marrow, compared to chimeric *Ldlr*$^{-/-}$ mice reconstituted with *LysM*$^{Cre-}$*Egfr*$^{lox/lox}$ bone marrow, after 4 weeks (-43%, $P<0.05$), 7 weeks (-34%, $P<0.05$), and 12 weeks (-54%, $P<0.001$) of high fat diet. Reduction of lesion size was associated with marked reduction in macrophage accumulation and necrotic core size. Specific deletion of *Egfr* in myeloid cells reduced TNF-α and IL-6 production by stimulated macrophages but had no effect on IL-10 and IL-12p70 secretion. Finally, we found that myeloid deletion of *Egfr* limited cytoskeletal rearrangements and also lipid up-take by macrophages through a down-regulation of the scavenger receptor CD36.

Conclusion. Gene deletion of *Egfr* in myeloid cells limits IL-6 and TNF-α production, lipid uptake, and consecutively reduces atherosclerosis development

Key words: Atherosclerosis, inflammation, macrophage, foam cell, EGFR.

Non standard abbreviations and Acronyms	
BMDM	Bone marrow-derived macrophages
CD	Cluster of differentiation
EGFR	Epidermal growth factor receptor
IFN	Interferon
IL-	Interleukin-
LDLr	Low density lipoprotein receptor
LPS	Lipopolysaccharide
MOMA	Monocyte-macrophage marker
MSR	Macrophage scavenger receptor
PPAR	Peroxisome proliferator-activated receptor
TKI	Tyrosine kinase inhibitor
TLR	Toll-like receptor
TNF	Tumor necrosis factor

Introduction

Atherosclerosis is a Western life-style associated inflammatory disease of the arterial wall responsible for ischemic cardiovascular diseases and stroke [1]. There is a large body of human and experimental evidences showing that innate immunity plays a crucial role in atherosclerosis development and complications. Monocyte-derived macrophages of the intima internalize and are activated by a broad range of molecules and particles bearing damage-associated molecular patterns (e.g., oxidized LDL), and ultimately are transformed into pro-inflammatory foam cells. Macrophage maturation, activation and proliferation are necessary steps for atherosclerosis and are associated with up-regulation of pattern recognition receptors for innate immunity, including scavenger receptors (SR-A, CD36) and toll-like receptors (TLR) [2-4]. Modulating monocyte/macrophage pathogenic function could represent an interesting therapeutic approach to limit atherosclerosis development and complications, and to stop the burden of cardiovascular diseases.

The epidermal growth factor receptor (EGFR) is a prominent member of the receptor tyrosine kinase family [5]. EGFR and its ligands have been detected in atherosclerotic plaques of mice [6], rabbits, monkeys [7] and humans [8-10], colocalizing with vascular smooth muscle cells and macrophages. EGFR phosphorylation has been documented in aortas of athero-prone *Apoe*$^{-/-}$ mice under a high fat diet, and repetitive administration of AG-1478, a tyrosine kinase inhibitor (TKI) specific for EGFR, reduced atherosclerosis in *Apoe*$^{-/-}$ mice [11]. However, since EGFR is expressed by vascular (endothelial and smooth muscle), myeloid and T cells, the atheroprotective effects of TKI cannot be directly ascribed to the modulation of a specific cell population, in particular monocytes/macrophages. To investigate the specific *in vivo* consequences of EGFR blockade in myeloid cell function, we generated a cell-specific deletion of *Egfr* and performed bone marrow transplantation experiments in irradiated *Ldlr*$^{-/-}$ mice.

Materials and Methods

Materials and Methods are available in the online-only Data Supplement.

Results

First of all, we searched for EGFR expression in plaques of *Ldlr*$^{-/-}$ mice, an athero-prone model routinely used for bone marrow transplantation experiments. In adult males, after 4 weeks of high fat diet, EGFR was expressed in atherosclerotic lesions and colocalized with MOMA-2+ macrophages. After 8 weeks of high fat diet, in more advanced lesions, EGFR was mainly expressed around the lipid-rich necrotic area and colocalized with macrophages, although not exclusively (Figure I in the online-only Data Supplement), suggesting that other cell types may express EGFR in atherosclerotic lesions. We next assessed the specific role of EGFR activation in myeloid cells during the development of atherosclerosis. *LysM*$^{Cre+/}$*Egfr*$^{lox/lox}$ mice were obtained by crossing the *loxP*-flanked *Egfr* mice (*Egfr*$^{lox/lox}$) with mice expressing Cre recombinase under the control of the murine M lysozyme promoter, which is specific for cells of the myeloid lineage (*LysM*$^{cre+}$). *Egfr* deletion was confirmed in adherent peritoneal macrophages (Figure II in the online-only Data Supplement). Next, we performed bone marrow transplantation experiments using either *LysM*$^{Cre-}$*Egfr*$^{lox/lox}$ or *LysM*$^{Cre+}$*Egfr*$^{lox/lox}$ littermate bone marrow to repopulate lethally irradiated *Ldlr*$^{-/-}$ mice. After 4 weeks of recovery and additional 4 weeks on high fat diet, animals were euthanized. We did not observe any difference in animal or spleen weights between the 2 groups of mice (data not shown). Leukocyte populations (neutrophils, monocytes, B cells, T cells) were not different between groups, neither in the blood nor in the spleen (Figure III in the online-only Data Supplement). Egfr expression was detected in plaques of control chimeric mice but was not found in atherosclerotic plaques of *chimeric ldlr*$^{-/-}$*/LysM*$^{Cre+/}$*Egfr*$^{lox/lox}$ mice (Figure IV in the online-only Data Supplement). As shown in Figure 1A, *Egfr* deficiency in myeloid cells led to

a 43% decrease in atherosclerotic lesion size in the aortic sinus compared with controls (16 ± 6 x 10^3 μm^2 vs 28 ± 6 x 10^3 μm^2 $P<0.05$). The reduction of atherosclerosis was confirmed after 7 weeks (-34%, $P<0.05$) and 12 weeks (-54%, $P<0.001$) of high fat diet. Plasma cholesterol levels were comparable between the groups of mice (Figure 1B).

Plaque composition was analyzed in advanced lesions of chimeric *Ldlr*$^{-/-}$ mice after 12 weeks of high fat diet. We found a decrease in both macrophage accumulation (Figure 1C) and necrotic core area (Figure 1D) in lesions of *LysM*$^{Cre+}$*Egfr*$^{lox/lox}$→ *Ldlr*$^{-/-}$ compared to *LysM*$^{Cre-}$ *Egfr*$^{lox/lox}$ → *Ldlr*$^{-/-}$ mice, but no difference regarding collagen content (Figure V in the online-only Data Supplement). Based on previous studies reporting that pharmacological inhibition of EGFR limits cytokine production in non-hypercholesterolemic context [12] [13], we investigated the immuno-inflammatory response in chimeric *Ldlr*$^{-/-}$ mice. LPS/IFN-γ-stimulated splenocytes showed a slight deviation toward an anti-inflammatory profile in *Ldlr*$^{-/-}$/*LysM*$^{Cre+}$*Egfr*$^{lox/lox}$ chimeric mice when compared to *Ldlr*$^{-/-}$/*LysM*$^{Cre-}$ *Egfr*$^{lox/lox}$ chimeric mice with a reduction of TNF-α production but no difference for IL-12p70 and IL-10 (ELISA, Figure 2A). The expression of *Il10, Il12p70 and Tnf* mRNAs in the spleens was not different between groups (Figure 2A). Furthermore, *Ldlr*$^{-/-}$/*LysM*$^{Cre+}$*Egfr*$^{lox/lox}$ bone marrow-derived macrophages were less prone to polarize toward a pro-inflammatory phenotype after LPS/IFN-γ, as they produced less of TNF-α and less of IL-6 (ELISA, Figure 2A). In order to gain insight into the mechanisms of reduction of macrophage and necrotic core content in *Ldlr*$^{-/-}$ mice reconstituted with *LysM*$^{Cre+}$*Egfr*$^{lox/lox}$ bone marrow, we first evaluated cell death. *In vitro*, apoptosis susceptibility of macrophages was comparable between the 2 genetic backgrounds after serum deprivation or exposure to TNF-α/cycloheximide (Figure VI in the online-only Data Supplement). We hypothesized that the marked reduction of Oil red O+ lesions in *Ldlr*$^{-/-}$/*LysM*$^{Cre+}$*Egfr*$^{lox/lox}$ mice could be due, at least in part, to a reduction of foam cell formation. To explore this hypothesis, we performed *in vitro* experiments to examine the

uptake of oxidized LDL by BMDMs and their ability to accumulate intracellular lipids. Interestingly, lipid uptake was significant reduced in *LysM^{Cre+}Egfr$^{lox/lox}$* cultured macrophages and in AG-1478-treated *LysM^{Cre-}Egfr$^{lox/lox}$* macrophages in comparison with control *LysM^{Cre-}Egfr$^{lox/lox}$* macrophages after 24 hours of incubation with oxLDL (figure 2B). This result was confirmed in peritoneal macrophages (Figure VII in the online-only Data Supplement). In addition, we found that AG-1478 treatment reduced cholesterol content in macrophages exposed to oxidized LDL (Figure VIII in the online-only Data Supplement). We found no difference in *Abca1, Abcg1* (Figure IX in the online-only Data Supplement), *Scarb1 and Msr1 mRNA* expression between groups (Figure 2C). However, we identified a reduction of *Cd36 mRNA* expression in *LysM^{Cre+}Egfr$^{lox/lox}$* cultured macrophages after stimulation with oxLDL (Figure 2C). A reduction of CD36 protein was further confirmed by flow cytometry (Figure 2D). Pharmacological inhibition of EGFR using AG-1478 reduced oxidized LDL endocytosis in *C57Bl6* control macrophages but had no effect on lipid uptake in *Cd36$^{-/-}$* cells suggesting that EGFR controls lipid uptake through the regulation of CD36 expression (Figure 2E). Finally, to evaluate the *in vivo* relevance of our data, we stained and quantified CD36 protein expression in plaques from chimeric *Ldlr$^{-/-}$* mice. CD36 was detected in atherosclerotic plaques and co-localized with MOMA-2 (Figure X in the online-only Data Supplement). We found a profound decrease of CD36 staining in atherosclerotic plaques of chimeric *Ldlr$^{-/-}$* mice retransplanted with *LysM^{Cre+}Egfr$^{lox/lox}$* bone marrow cells (Figure 2F and Figure X in the online-only Data Supplement). As EGFR could interact with Focal Adhesion Kinase [14] and CD36 is involved in cell migration [15], we hypothesized that the atheroprotection induced by EGFR deficiency in myeloid cells could also be due, in part, to impairment of cytoskeleton rearrangements. In vitro, we found that Egfr deficiency limited monocyte adhesion to serum coated coverslips and also limited macrophage spreading and actin polymerization when exposed to oxLDL (Figure XI in the online-only Data Supplement).

Discussion

In this study, we showed that selective deletion of *Egfr* in myeloid cells reduced atherosclerosis development, limiting both lipid uptake and the inflammatory response.

Our study extends previous findings by highlighting the role of EGFR engagement on the inflammatory response of macrophages in the context of atherosclerosis [11]. Genetic deficiency of *Egfr* in myeloid cells modulated the systemic innate inflammatory response as illustrated by the reduction of pro-atherogenic TNF-α production by both splenocytes and macrophages after TLR4 agonist stimulation [3, 16]. Our result are consistent with the recent study by Wang et al. who reported a reduction of TNF-α and IL-6 production by OxLDL-stimulated macrophages after incubation with 2 different pharmacological EGFR inhibitors [11].

Given the strong reduction of the area of aortic Oil red O staining in the absence of myeloid EGFR, we investigated the role of EGFR in macrophage foam cell formation and found a marked reduction of oxidized LDL uptake and lipid accumulation in *Egfr* deficient macrophages. Among the major receptors that govern foam cell formation in macrophages (i.e., MSR1, CD36), *Egfr* deletion selectively altered the expression of CD36 both at the gene and cell surface protein expression levels, and both *in vitro* and within atherosclerotic plaque macrophages *in vivo*. Our results are in agreement with previous *in vitro* work that showed reduced lipid uptake by both mouse [11] and human [17] macrophages treated with an EGFR tyrosine kinase inhibitor. In addition, we found that AG-1478 had no effect on lipid uptake in *Cd36*$^{-/-}$ macrophages suggesting that CD36 is the main regulatory mechanism of lipid uptake driven by the EGFR pathway. We did not investigate downstream pathways but we speculate that PPAR-γ might be involved given its major impact on CD36 expression and its regulation by the EGFR pathway [18].

EGFR is also expressed by polymorphonuclear cells [19] and we cannot exclude a contribution of neutrophils to the vascular phenotype observed in chimeric *Ldlr*$^{-/-}$/*LysM*$^{Cre+}$*Egfr*$^{lox/lox}$. However, such a contribution is probably minor because previous studies that used anti-GR1 depleting strategy reported a proatherogenic role of neutrophils at early stages of atherosclerosis but no significant effect in advanced plaques [20]. Here, we reported that myeloid EGFR deficiency was protective at both early and late stages of atherosclerosis development.

Conclusion

Selective deletion of EGFR in myeloid cells reduced atherosclerosis and plaque inflammation. Our findings suggest that targeting of EGFR pathway could be an interesting therapeutic strategy to limit plaque growth and promote plaque stability.

Acknowledgements

This work was supported by Institut National de la Santé et de la Recherche Médicale (INSERM) and the British Heart Foundation (Z.M).

Authors Contributions

Study concept and design, all authors. Acquisitions of data LZ, AG, LG, YZ, LL, BE, AC, NPM, CJB, JV and HAO. Drafting of the manuscript LZ, AT, ZM, PLT and HAO. Critical revision of manuscript, all the authors. Statistical analysis, LZ and HAO.

Disclosures

None

References

1. Hansson, G.K. Inflammation, atherosclerosis, and coronary artery disease. N Engl J Med. 2005; **352**: 1685-95.
2. Libby, P. Inflammation in atherosclerosis. Nature. 2002; **420**: 868-74.
3. Ait-Oufella, H., Taleb, S., Mallat, Z., and Tedgui, A. Recent advances on the role of cytokines in atherosclerosis. Arterioscler Thromb Vasc Biol. 2011; **31**: 969-79.
4. Robbins, C.S., Hilgendorf, I., Weber, G.F., Theurl, I., Iwamoto, Y., Figueiredo, J.L., Gorbatov, R., Sukhova, G.K., Gerhardt, L.M., Smyth, D., Zavitz, C.C., Shikatani, E.A., Parsons, M., van Rooijen, N., Lin, H.Y., Husain, M., Libby, P., Nahrendorf, M., Weissleder, R., and Swirski, F.K. Local proliferation dominates lesional macrophage accumulation in atherosclerosis. Nat Med. 2013; **19**: 1166-72.
5. Lemmon, M.A. and Schlessinger, J. Cell signaling by receptor tyrosine kinases. Cell. 2010; **141**: 1117-34.
6. Gao, P., Wang, X.M., Qian, D.H., Qin, Z.X., Jin, J., Xu, Q., Yuan, Q.Y., Li, X.J., and Si, L.Y. Induction of oxidative stress by oxidized LDL via meprinalpha-activated epidermal growth factor receptor in macrophages. Cardiovasc Res. 2013; **97**: 533-43.
7. Stanic, B., Pandey, D., Fulton, D.J., and Miller, F.J., Jr. Increased epidermal growth factor-like ligands are associated with elevated vascular nicotinamide adenine dinucleotide phosphate oxidase in a primate model of atherosclerosis. Arterioscler Thromb Vasc Biol. 2012; **32**: 2452-60.
8. Miyagawa, J., Higashiyama, S., Kawata, S., Inui, Y., Tamura, S., Yamamoto, K., Nishida, M., Nakamura, T., Yamashita, S., Matsuzawa, Y., and et al. Localization of heparin-binding EGF-like growth factor in the smooth muscle cells and macrophages of human atherosclerotic plaques. J Clin Invest. 1995; **95**: 404-11.
9. Nakata, A., Miyagawa, J., Yamashita, S., Nishida, M., Tamura, R., Yamamori, K., Nakamura, T., Nozaki, S., Kameda-Takemura, K., Kawata, S., Taniguchi, N., Higashiyama, S., and Matsuzawa, Y. Localization of heparin-binding epidermal growth factor-like growth factor in human coronary arteries. Possible roles of HB-EGF in the formation of coronary atherosclerosis. Circulation. 1996; **94**: 2778-86.
10. Dreux, A.C., Lamb, D.J., Modjtahedi, H., and Ferns, G.A. The epidermal growth factor receptors and their family of ligands: their putative role in atherogenesis. Atherosclerosis. 2006; **186**: 38-53.
11. Wang, L., Huang, Z., Huang, W., Chen, X., Shan, P., Zhong, P., Khan, Z., Wang, J., Fang, Q., Liang, G., and Wang, Y. Inhibition of epidermal growth factor receptor attenuates atherosclerosis via decreasing inflammation and oxidative stress. Sci Rep. 2017; **8**: 45917.
12. Hardbower, D.M., Singh, K., Asim, M., Verriere, T.G., Olivares-Villagomez, D., Barry, D.P., Allaman, M.M., Washington, M.K., Peek, R.M., Jr., Piazuelo, M.B., and Wilson, K.T. EGFR regulates macrophage activation and function in bacterial infection. J Clin Invest. 2016; **126**: 3296-312.
13. Srivatsa, S., Paul, M.C., Cardone, C., Holcmann, M., Amberg, N., Pathria, P., Diamanti, M.A., Linder, M., Timelthaler, G., Dienes, H.P., Kenner, L., Wrba, F., Prager, G.W., Rose-John, S., Eferl, R., Liguori, G., Botti, G., Martinelli, E., Greten, F.R., Ciardiello, F., and Sibilia, M. EGFR in Tumor-Associated Myeloid Cells Promotes Development of Colorectal Cancer in Mice and Associates With Outcomes of Patients. Gastroenterology. 2017.
14. Tai, Y.L., Chu, P.Y., Lai, I.R., Wang, M.Y., Tseng, H.Y., Guan, J.L., Liou, J.Y., and Shen, T.L. An EGFR/Src-dependent beta4 integrin/FAK complex contributes to malignancy of breast cancer. Sci Rep. 2015; **5**: 16408.

15. Park, Y.M., Febbraio, M., and Silverstein, R.L. CD36 modulates migration of mouse and human macrophages in response to oxidized LDL and may contribute to macrophage trapping in the arterial intima. J Clin Invest. 2009; **119**: 136-45.
16. Tedgui, A. and Mallat, Z. Cytokines in atherosclerosis: pathogenic and regulatory pathways. Physiol Rev. 2006; **86**: 515-81.
17. Osada-Oka, M., Kita, H., Yagi, S., Sato, T., Izumi, Y., and Iwao, H. Angiotensin AT1 receptor blockers suppress oxidized low-density lipoprotein-derived formation of foam cells. Eur J Pharmacol. 2012; **679**: 9-15.
18. Slomiany, B.L. and Slomiany, A. Role of epidermal growth factor receptor transactivation in PPAR gamma-dependent suppression of Helicobacter pylori interference with gastric mucin synthesis. Inflammopharmacology. 2004; **12**: 177-88.
19. Lewkowicz, P., Tchorzewski, H., Dytnerska, K., Banasik, M., and Lewkowicz, N. Epidermal growth factor enhances TNF-alpha-induced priming of human neutrophils. Immunol Lett. 2005; **96**: 203-10.
20. Drechsler, M., Megens, R.T., van Zandvoort, M., Weber, C., and Soehnlein, O. Hyperlipidemia-triggered neutrophilia promotes early atherosclerosis. Circulation. 2010; **122**: 1837-45.

Highlights

Specific deletion of *Egfr* in myeloid cells:

- reduced TNF-α and IL-6 production by macrophages

- limited lipid up-take by macrophages through a down-regulation of the scavenger receptor CD36.

- reduced atherosclerosis development and induced a more stable plaque phenotype

Figure legends

Figure 1. ***Egfr*** **deletion in myeloid cells reduces atherosclerosis in chimeric** ***Ldlr*** $^{-/-}$ **mice and limits macrophage accumulation.** A, representative photomicrographs and quantitative analysis of atherosclerotic lesions of chimeric *Ldlr* $^{-/-}$ mice after 4, 7 and 12 weeks of high fat diet. Scale bar 200 μm. B, Plasma cholesterol level of *Ldlr* $^{-/-}$ chimeric mice after 4, 7 and 12 weeks of fat diet. C, representative photomicrographs and quantitative analysis of macrophage accumulation (MOMA staining) in atherosclerotic lesions of chimeric *Ldlr* $^{-/-}$ mice after 12 weeks of fat diet. D, representative photomicrographs and quantitative analysis of acellular area (Masson's Trichrome) of chimeric *Ldlr* $^{-/-}$ mice after 12 weeks of fat diet. * $P<0.05$. ** $P<0.01$, non-parametric Mann-Whitney test. Scale bar 70 μm.

Figure 2. Myeloid ***Egfr*** **deletion inhibits pro-inflammatory innate immune responses and lipid uptake.** A, Cytokine production (ELISA) by LPS/IFNγ-stimulated splenocytes isolated from chimeric *Ldlr* $^{-/-}$ mice after 4 weeks of high fat diet; quantification of cytokine *mRNA* expression in spleens of chimeric *Ldlr* $^{-/-}$ mice (related to *Gapdh*); cytokine production (ELISA) by LPS/IFNγ-stimulated bone marrow-derived macrophages (BMDMs) isolated from *Ldlr* $^{-/-}$ chimeric mice, after 4 weeks of high fat diet. B, Representative photomicrographs and quantitative analysis of lipid-laden macrophages after incubation of BMDMs from *LysM* $^{Cre-}$*Egfr* $^{lox/lox}$ and *LysM* $^{Cre+}$*Egfr* $^{lox/lox}$ mice with oxLDL during 24h. C, Quantification of *Cd36*, *Msr1 and Scarb1 mRNAs* in BMDMs from *LysM* $^{Cre-}$*Egfr* $^{lox/lox}$ and *LysM* $^{Cre+}$*Egfr* $^{lox/lox}$ mice at baseline and after stimulation with oxLDL (related to *Gapdh*). D, flow cytometry quantification (Mean Fluorescence Intensity) of CD36 expression by BMDMs from *LysM* $^{Cre-}$ *Egfr* $^{lox/lox}$ and *LysM* $^{Cre+}$*Egfr* $^{lox/lox}$ mice after stimulation with oxLDL. E, Representative photomicrographs and quantitative analysis of lipid-laden macrophages after incubation of BMDMs from *Wild-type* and *Cd36* $^{-/-}$ mice with oxLDL during 24h +/- AG-1478 (10 μMol).

F, Representative photomicrographs and quantification of CD36 expression in plaques from chimeric *Ldlr*$^{-/-}$/*LysM*$^{Cre-}$*Egfr*$^{lox/lox}$ and *Ldlr*$^{-/-}$/*LysM*$^{Cre+}$*Egfr*$^{lox/lox}$ and mice. Scale bar 50 μm. * P<0.05. ** P<0.01. Non-parametric Mann-Whitney test was used in Figures 2A, C, D, F. Kruskal-Wallis test with post-hoc analysis was used in Figures 2B and E.

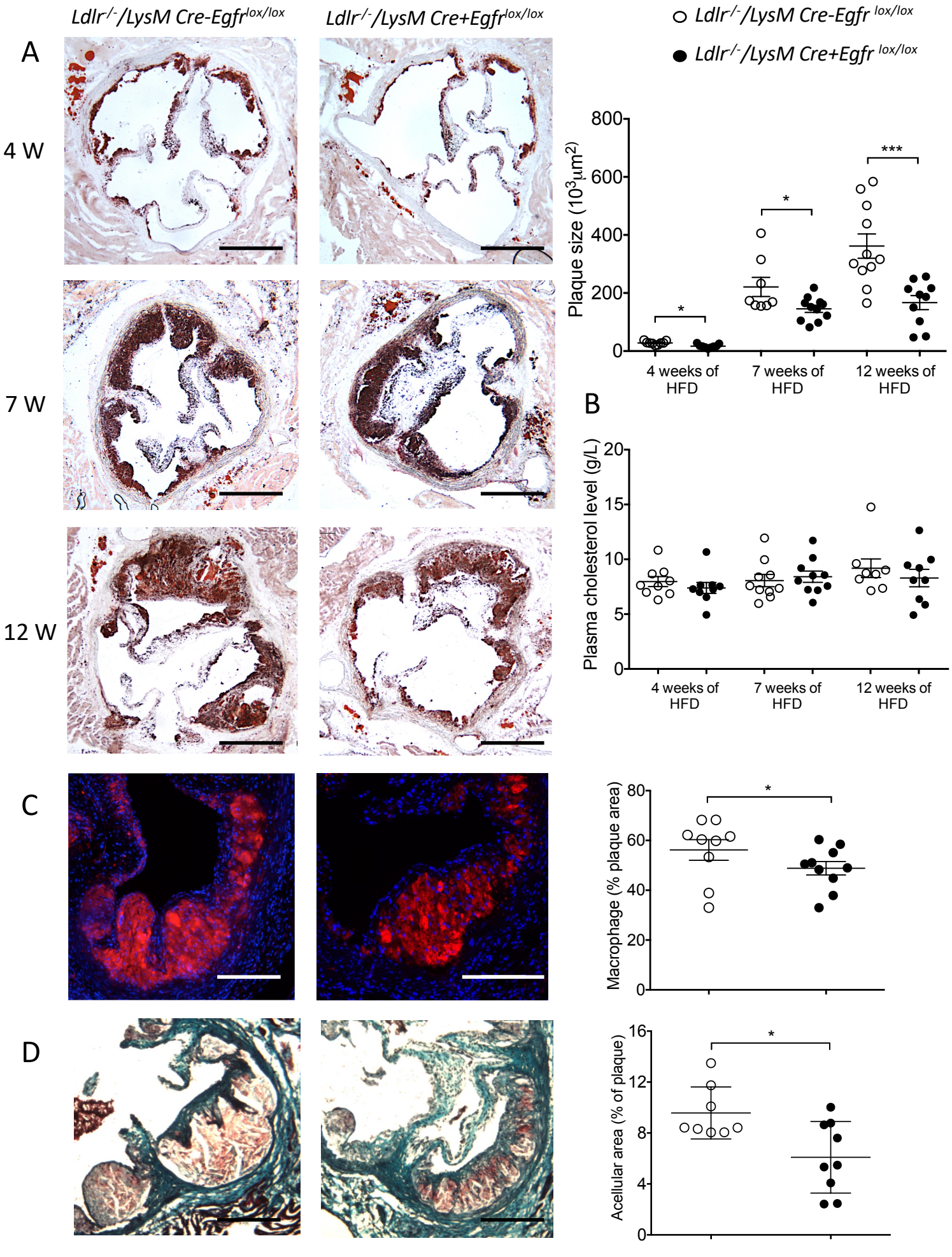
Ldlr-/-/LysM Cre-Egfrlox/lox
Ldlr-/-/LysM Cre+Egfrlox/lox
A
4 W
7 W
12 W
Ldlr-/-/LysM Cre-Egfr lox/lox
Ldlr-/-/LysM Cre+Egfr lox/lox
Plaque size (10³µm²)
800
600
400
200
0
*
*
***
4 weeks of HFD
7 weeks of HFD
12 weeks of HFD
B
Plasma cholesterol level (g/L)
20
15
10
5
0
4 weeks of HFD
7 weeks of HFD
12 weeks of HFD
C
Macrophage (% plaque area)
80
60
40
20
0
*
D
Acellular area (% of plaque)
16
12
8
4
0
*

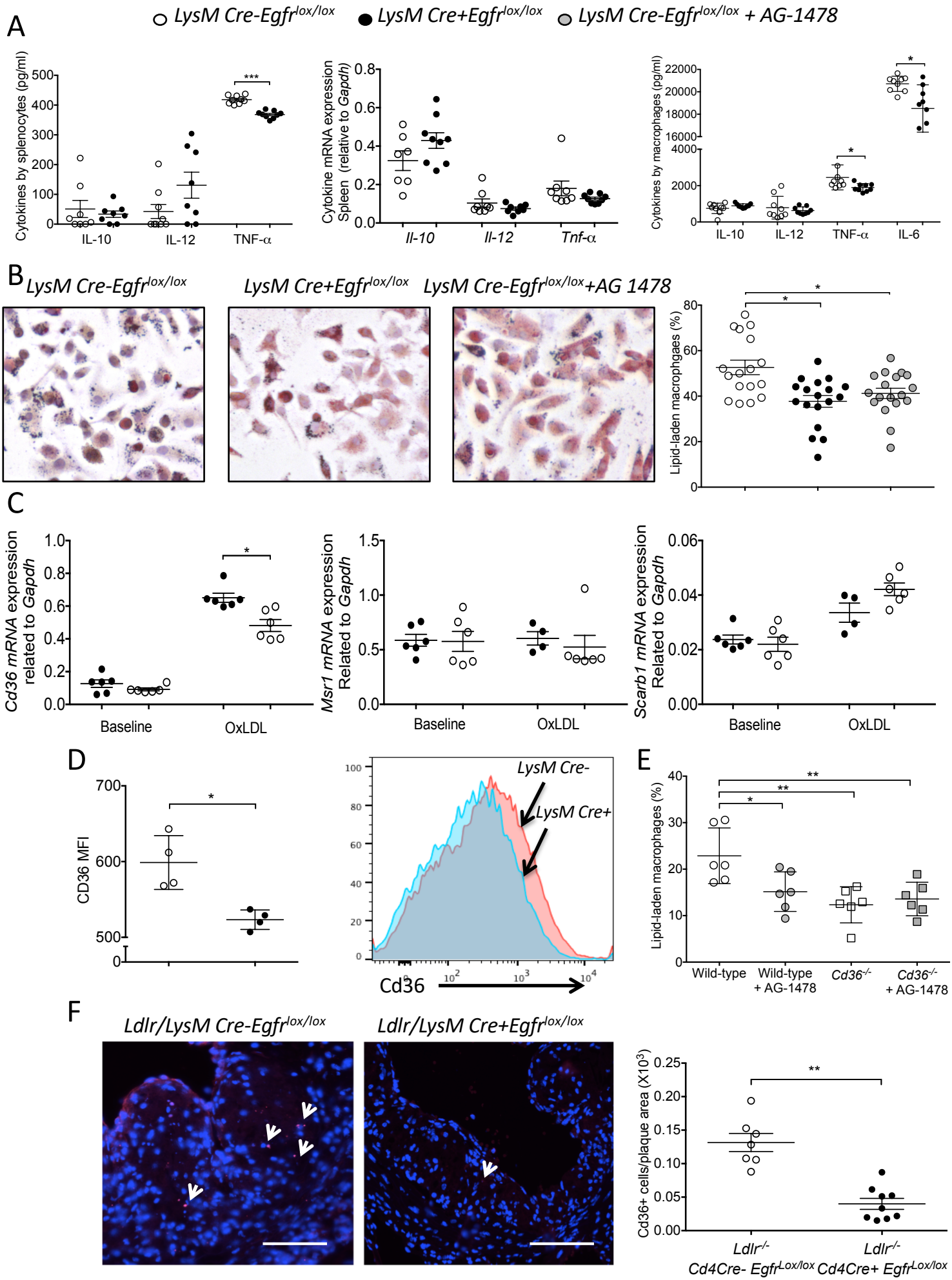
A
LysM Cre-Egfr lox/lox
LysM Cre+Egfr lox/lox
LysM Cre-Egfr lox/lox + AG-1478
Cytokines by splenocytes (pg/ml)
IL-10
IL-12
TNF-α
Cytokine mRNA expression Spleen (relative to Gapdh)
Il-10
Il-12
Tnf-α
Cytokines by macrophages (pg/ml)
IL-6
B
LysM Cre-Egfr lox/lox
LysM Cre+Egfr lox/lox
LysM Cre-Egfr lox/lox+AG 1478
Lipid-laden macrophgaes (%)
C
Cd36 mRNA expression related to Gapdh
Msr1 mRNA expression Related to Gapdh
Scarb1 mRNA expression Related to Gapdh
Baseline
OxLDL
D
CD36 MFI
LysM Cre-
LysM Cre+
Cd36
E
Lipid-laden macrophages (%)
Wild-type
Wild-type + AG-1478
Cd36-/-
Cd36-/- + AG-1478
F
Ldlr/LysM Cre-Egfr lox/lox
Ldlr/LysM Cre+Egfr lox/lox
Cd36+ cells/plaque area (X10³)
Ldlr-/- Cd4Cre- Egfr Lox/lox
Ldlr-/- Cd4Cre+ Egfr Lox/lox

Supplemental figure I

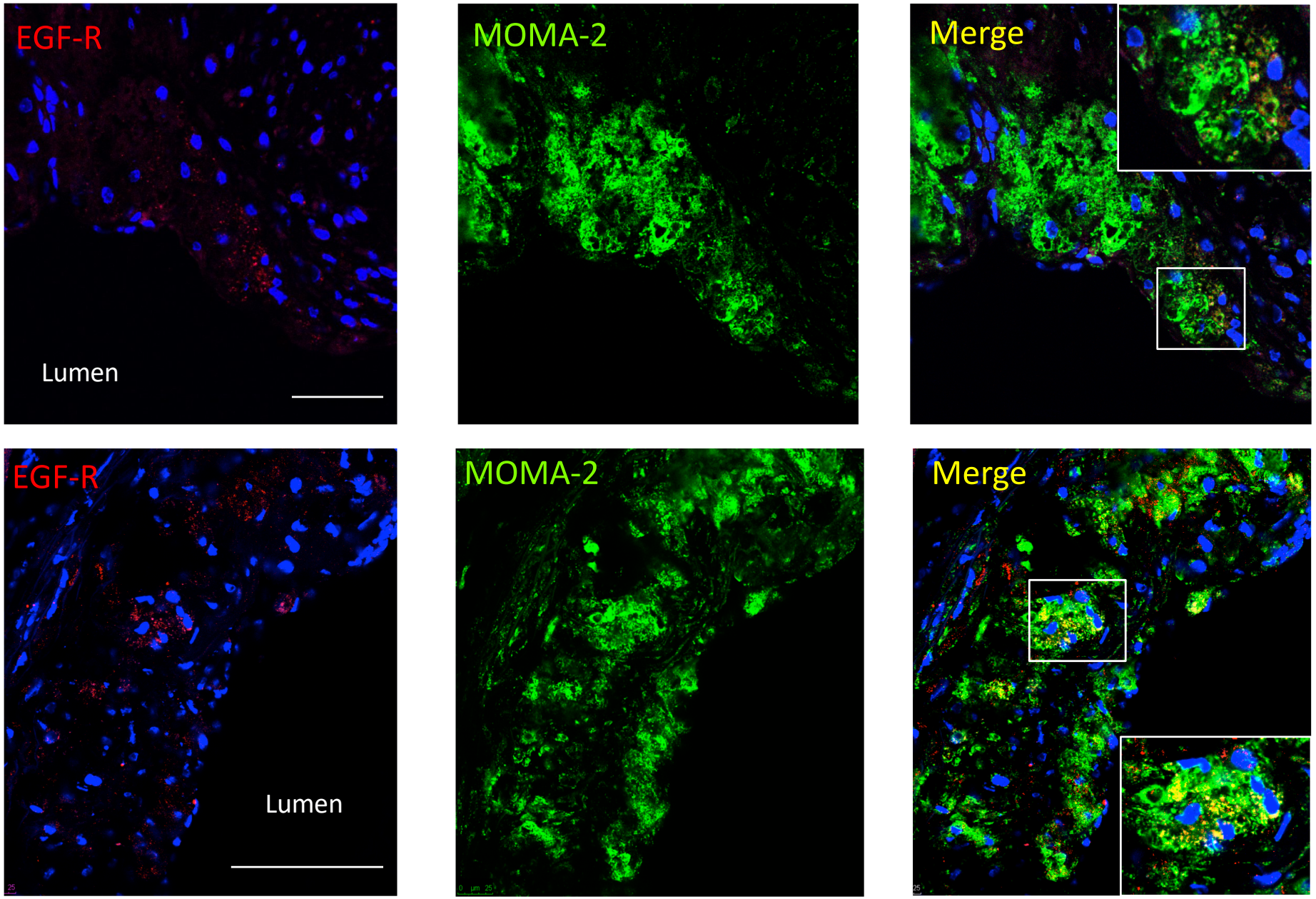

Egfr is expressed in atherosclerotic plaques of *Ldlr* $^{-/-}$ mice under at early stage (4 weeks of fat diet, up) and advanced stage of the disease (8 weeks of fat diet, down). Egfr (red) is expressed in plaques of *ldlr*$^{-/-}$ and colocalizes (yellow) with MOMA^{+} macrophages (green). Bar scale 50 μm.

Supplemental figure II

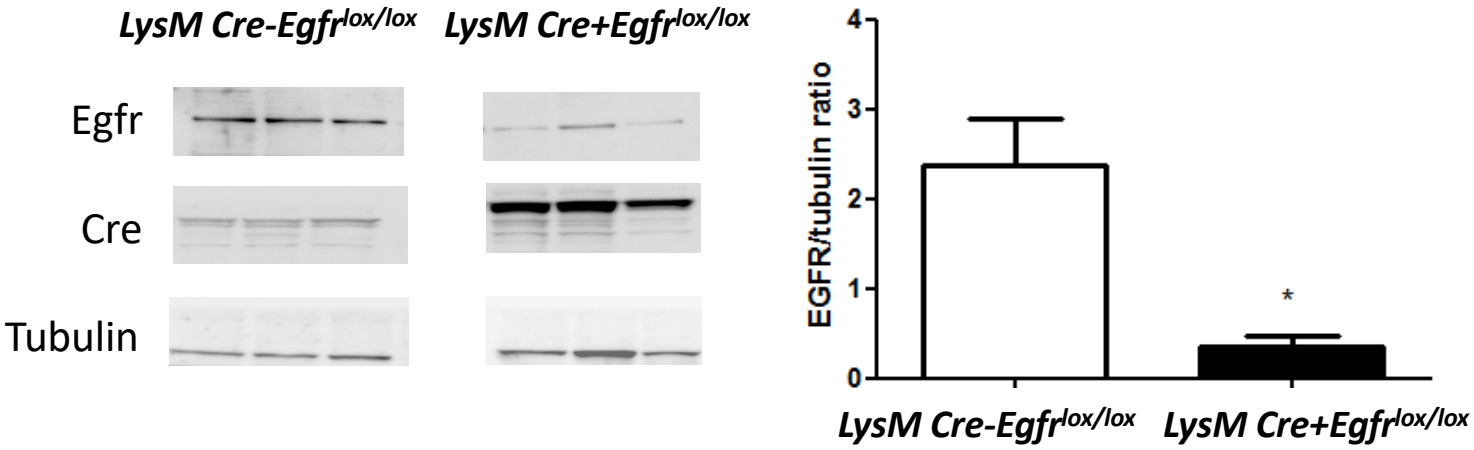

Egfr expression by peritoneal macrophages from *LysM Cre-Egfr$^{lox/lox}$* and *LysM Cre+Egfr$^{lox/lox}$* mice by Western Blot. Egfr expression related to tubulin. *, P<0.05

Supplemental figure III

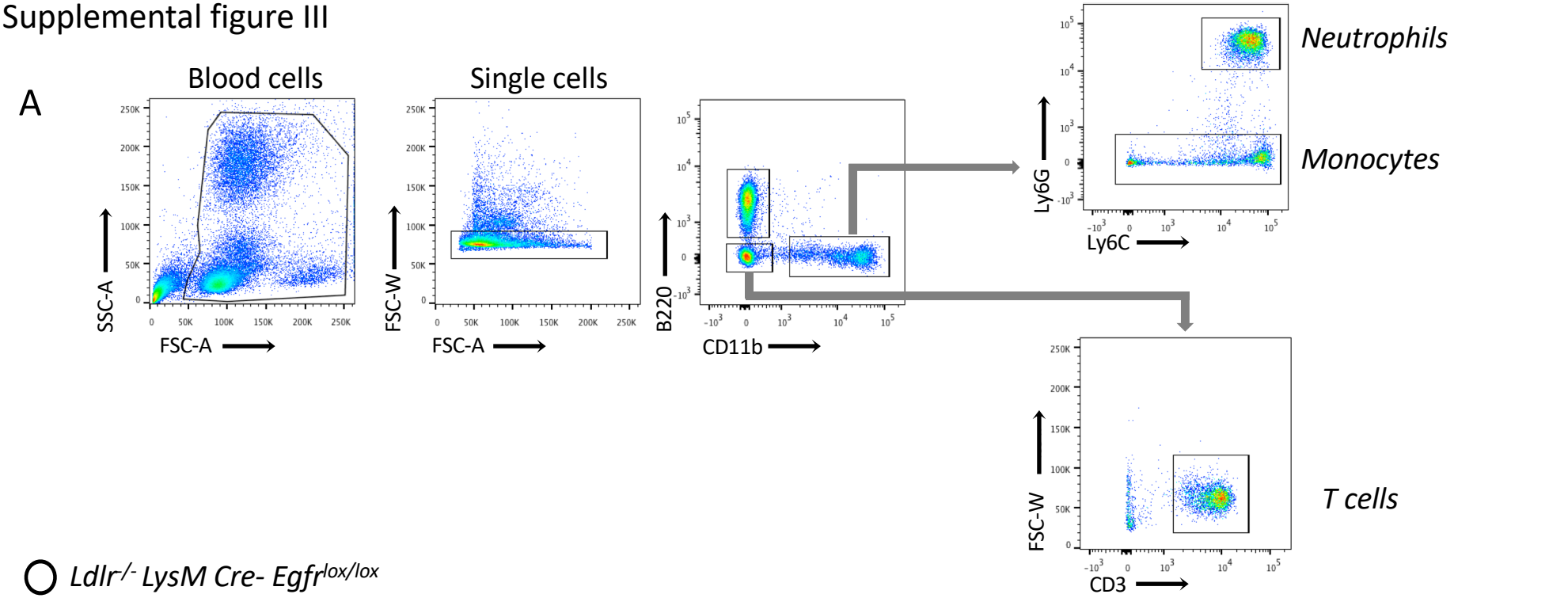

Flow cytometry characterization of leucocyte subsets in chimeric *Ldlr*$^{-/-}$ mice in the spleen after 4 weeks of high fat diet. Neutrophils were defined as Cd11b+Ly6G+ cells and monocytes as Cd11b+Ly6G-Ly6C+ cells.

Supplemental figure IV

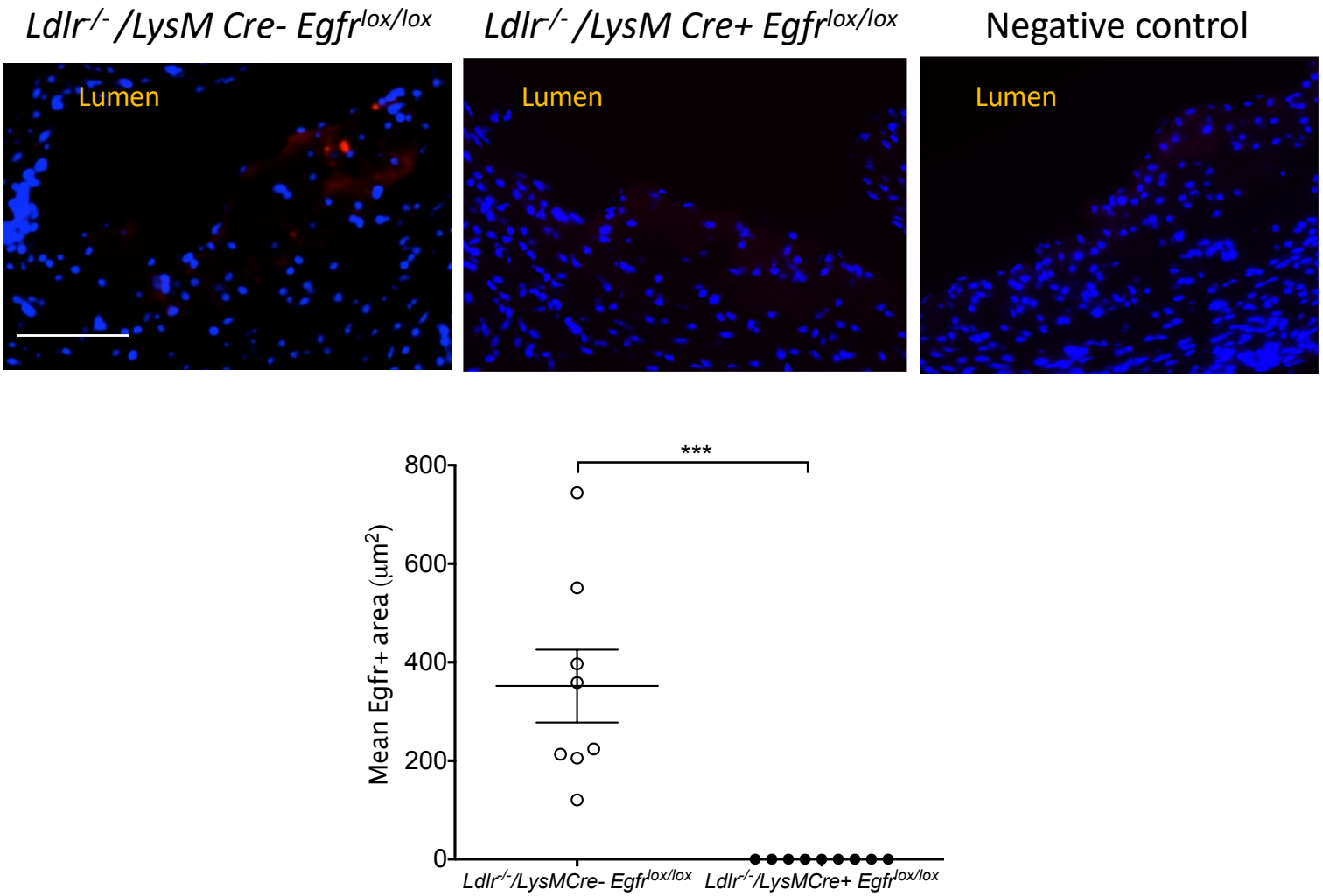

No expression of Egfr in atherosclerotic plaques of *Ldlr$^{-/-}$/LysM Cre+ Egfr$^{lox/lox}$*. Fluorescent staining and quantification (mean area, 4 sections/mouse) of Egfr in plaques of chimeric Ldlr$^{-/-}$ transplanted with bone marrow cells from LysM Cre+ Egfr$^{lox/lox}$ and control LysM Cre- Egfr$^{lox/lox}$ mice after 4 weeks of fat diet. Egfr was stained in Red, nuclei in Blue. Staining without primary antibody was called negative control. ***, P<0.001 Mann Whitney test. Bar scale 100 μm.

Supplemental figure V

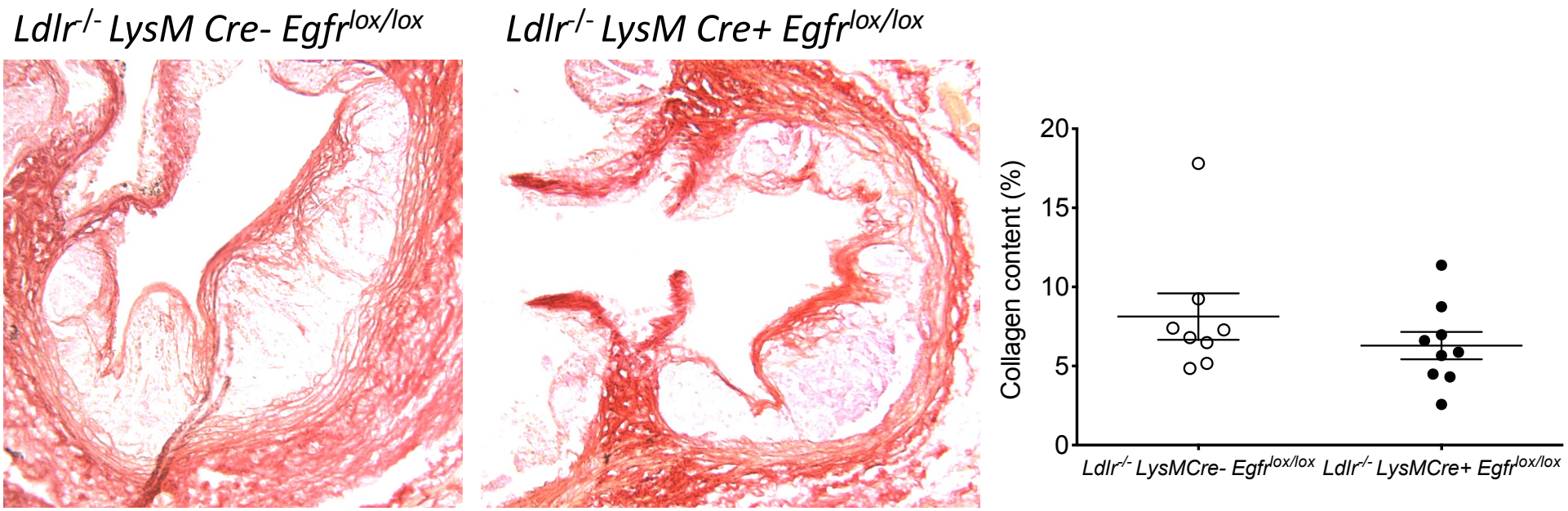

Representative photomicrographs and quantitative analysis of collagen content within atherosclerotic lesions of chimeric *Ldlr*$^{-/-}$ mice after 12 weeks of fat diet (Sirius red).

Supplemental figure VI

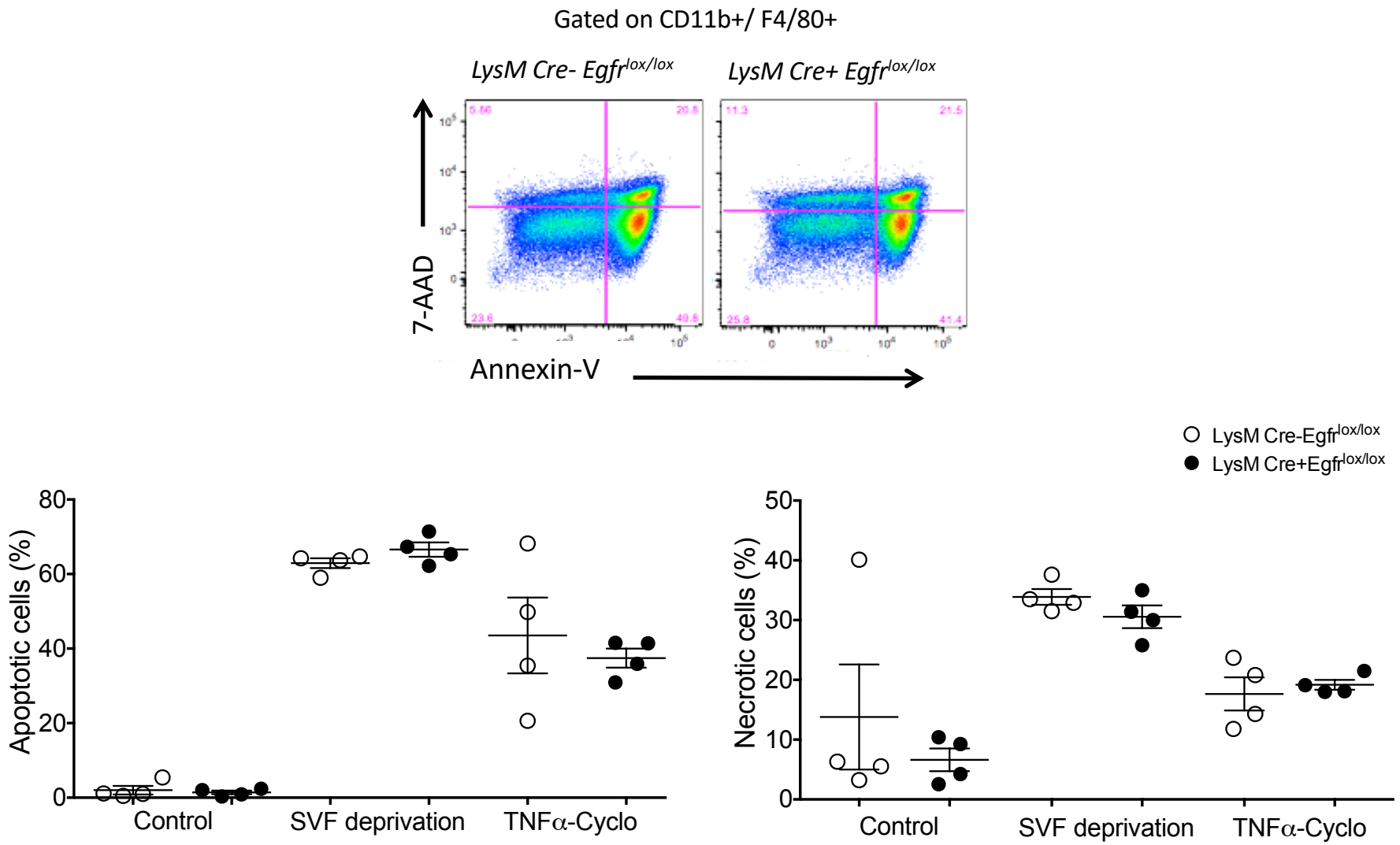

Bone marrow-derived macrophages isolated from *LysMCre- Egfr*$^{lox/lox}$ (opened circles) or *LysMCre+ Egfr*$^{lox/lox}$ mice (filled circles) were challenged *in vitro* during 24 hours and apoptosis was evaluated by flow cytometry. Apoptotic cells were defined as annexin V^{pos} 7-AAD^{neg} cells and necrotic cells were defined as annexin V^{pos} 7-AAD^{pos} cells.

Supplemental figure VII

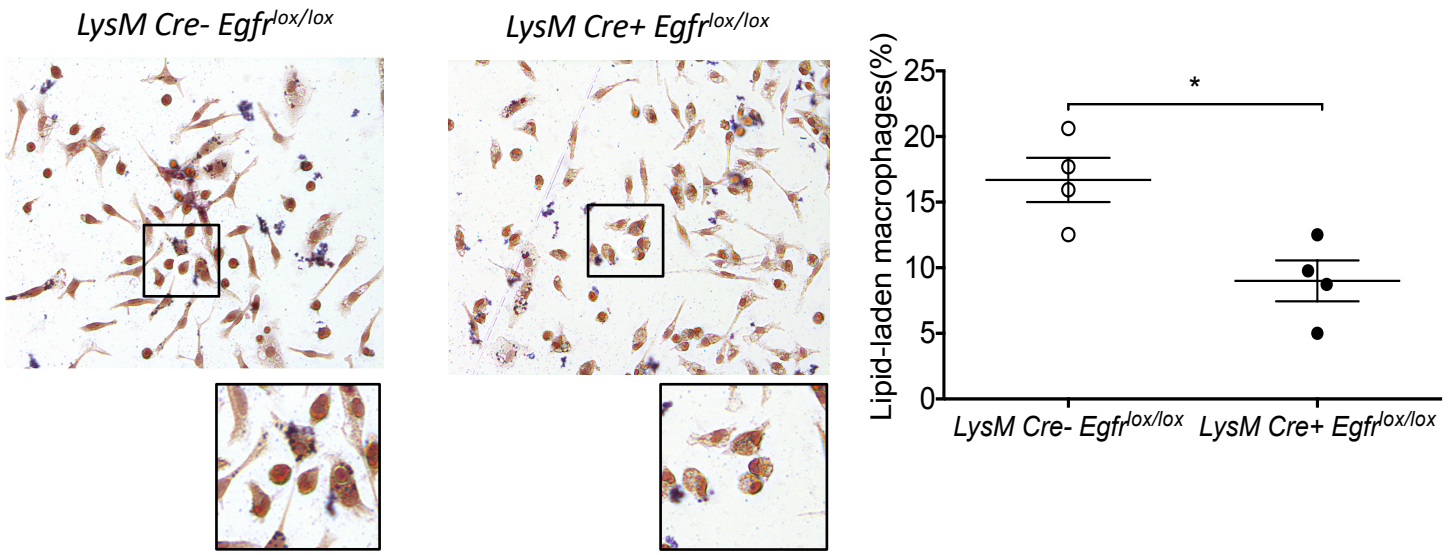

Representative photomicrographs and quantitative analysis of lipid uptake by peritoneal macrophages from *LysM Cre- Egfr$^{lox/lox}$* and *LysM Cre+ Egfr$^{lox/lox}$* mice with oxLDL during 24h. *, P<0.05, using non-parametric Mann-Whitney test.

Supplemental figure VIII

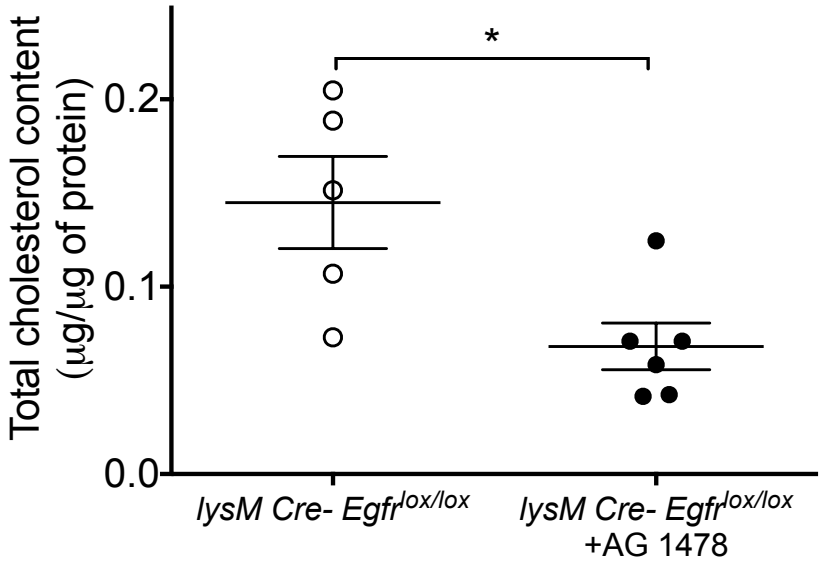

EGFR pharmacological inhibition reduced cholesterol content in oxidized LDL-stimulated macrophages. Quantification of cholesterol content (colorimetric assay Biomérieux, normalization to protein content) in BM-derived macrophages from control *LysM Cre- Egfr$^{lox/lox}$* mice cultured with oxLDL during 24h +/- AG-1478 (10 µMol), a pharmacological inhibitor of EGFR. *, P<0.05, using non-parametric Mann-Whitney test.

Supplemental figure IX

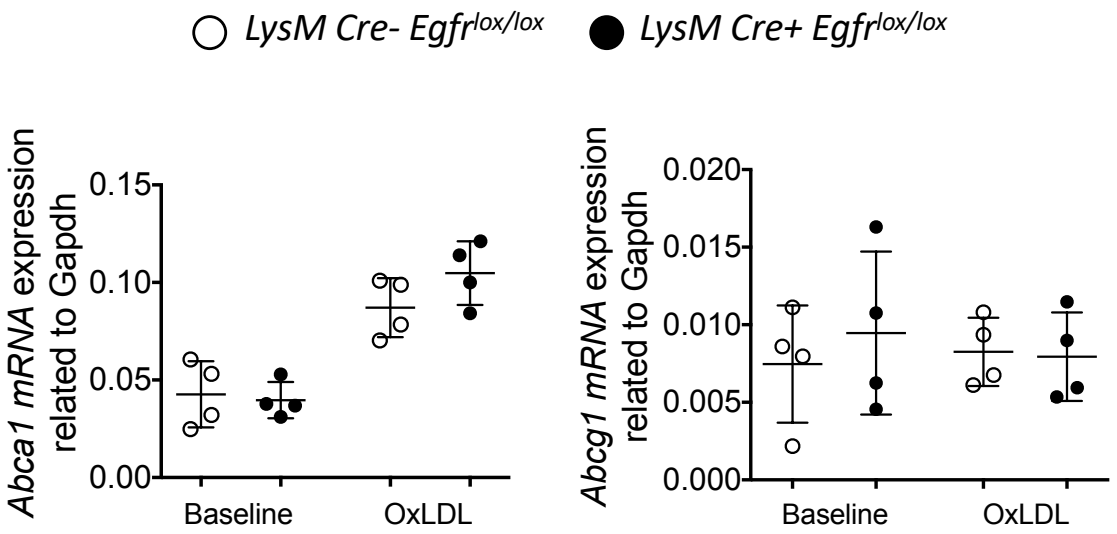

EGFR deficiency did not affect *Abca1* and *Abcg1* gene expression. Quantification of *Abca1 and Abcg1 mRNAs* in bone marrow-derived macrophages from *LysMCre- Egfr$^{lox/lox}$* and *LysMCre+ Egfr$^{lox/lox}$* mice at baseline and after stimulation with oxLDL (related to *Gapdh*).

Supplemental figure X

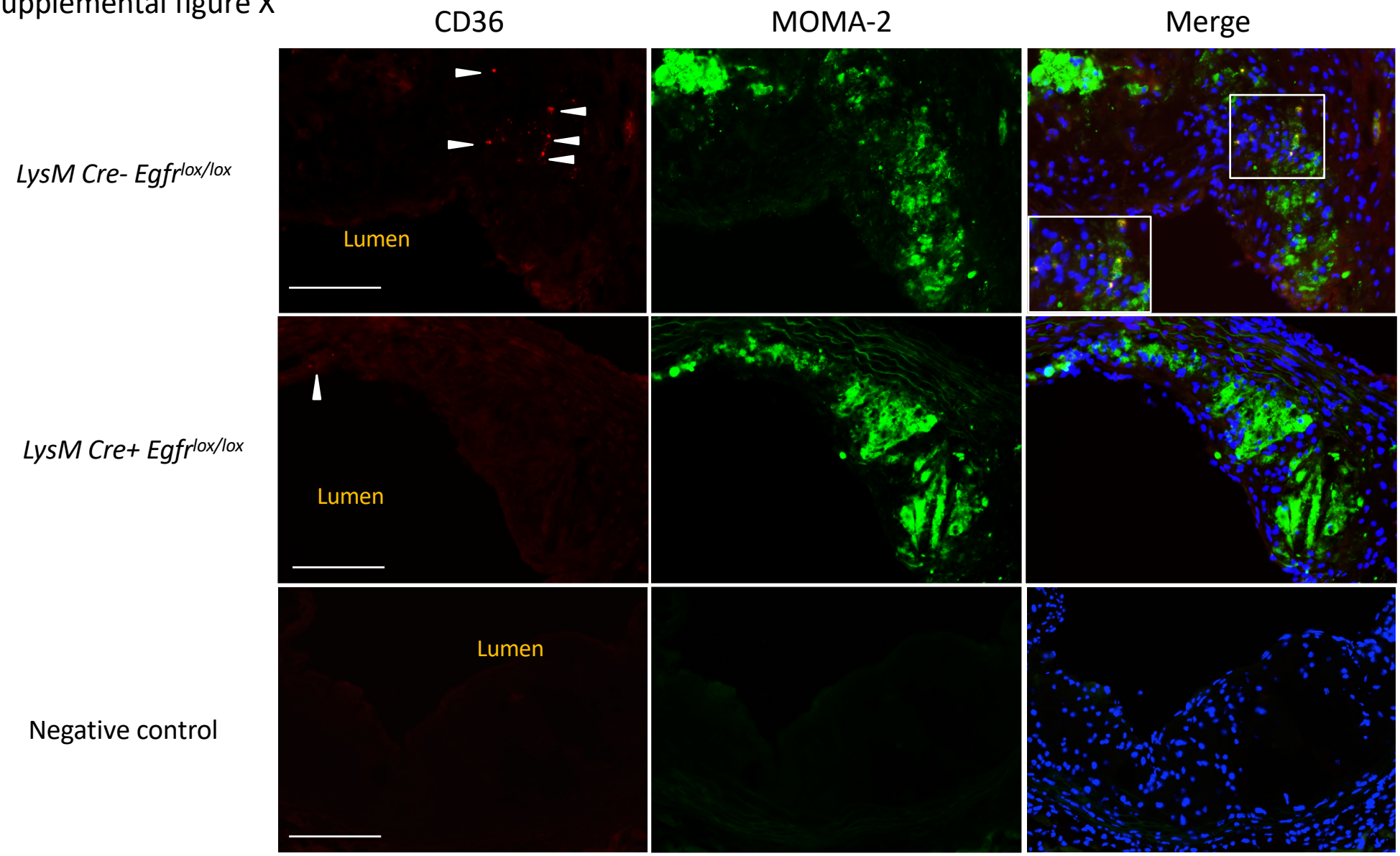

CD36 is expressed in atherosclerotic plaques of *chimeric Ldlr*$^{-/-}$ mice and colocalizes with macrophages. Fluorescent staining of CD36 (red) and Macrophages (MOMA-2, green) and colocalization (Yellow). Stainings without primary antibody are negative controls. Bar scale 50 μm.

Supplemental figure XI

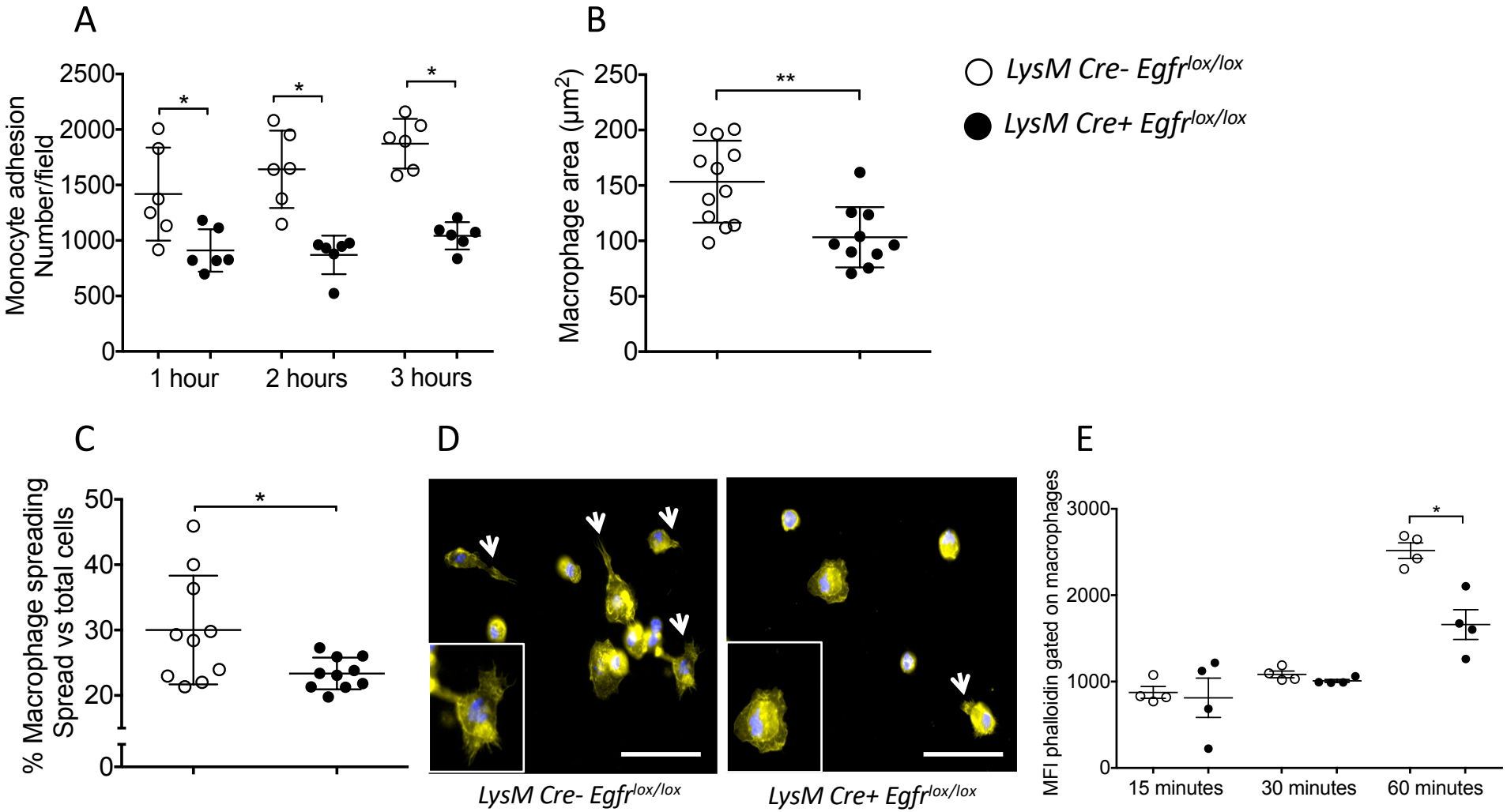

Egfr deficiency reduced monocyte adhesion, macrophage spreading and actin polymerization. Bone marrow (BM) monocytes were plated in serum coated coverslips during 1, 2 and 3 hours. After washing (X2) and DAPI staining, adherent monocytes were quantified (A). BM-derives macrophages were incubated with oxLDL during 1 hour and then fixed. Mean macrophage area (B) and cell spreading (C, D) were quantified blindly by confocal microscopy. Peritoneal macrophages (CD11b+F4/80+) were exposed to oxLDL and then stained with fluorescent-phalloidin to detect polymerized actin (E). *, P<0.05, ** P<0.01 Mann Whitney test.